High-Resolution Photonics-Based Interference Suppression Filter With Wide Passband

E. H. W. Chan and R. A. Minasian, *Fellow, IEEE*

***Abstract*—A new topology for a photonic signal processor, which overcomes the basic recursive frequency response problem that limits the passband range, is presented. The structure is based on a new multiple-wavelength offset-cavity structure that is cascaded with a series of unbalanced delay line structures. This not only can synthesize a very narrow notch response with good shape factor but also permits a multifold extension of the free spectral range (FSR) and passband width. Results on the interference mitigation filter demonstrate a stopband of 1% of center frequency and a fourfold increase in the FSR and passband width, while also having a very small shape factor, in excellent agreement with predictions.**

***Index Terms*—Gratings, notch filters, optical fiber delay lines, optical filters, optical signal processing.**

I. Introduction

PHOTONIC signal processing has attracted significant interest because of its high time-bandwidth potential and its ability to process microwave and radio-frequency (RF) signals directly within the optical fiber transport system. Photonics offers advantages of extremely wide bandwidth, electromagnetic interference immunity, and dense parallel signal-processing capabilities. The advantages of photonic processing, including the low-loss (independent of RF frequency) optical delay lines and the ability to provide very high sampling frequencies, beyond electronic capabilities, promises new microwave photonic transport systems with in-built signal conditioning.

Several photonic signal processor filter structures have been reported, e.g., [1]–[10]. However, all previously reported structures have a discrete-time signal-processor basis, and hence these filters have a recursive response, i.e., the design for a notch at a desired frequency f_0 also generates additional notches at lf_0, where l is an integer. This in turn limits the realizable width of the passband range. This limitation occurs for all existing photonic discrete time processing structures [1]–[10]. Thus the design frequency f_0 also sets the free spectral range (FSR) of the filter, which will limit the maximum attainable passband width of the filter, because the additional, unwanted notches at lf_0 come into effect at higher frequencies. This problem has not previously been solved.

In this paper, we report a new topology for a photonic signal processor that overcomes these limitations of a periodic frequency response. It enables both a high-resolution interference suppression filter and a very wide passband to be obtained. Our topology is based on a new multiple-wavelength offset-cavity structure that is cascaded with a series of unbalanced delay line structures. This not only can synthesize a very narrow notch response with good shape factor but also permits a fourfold extension of the FSR and passband width. Using this new topology, we present results for this photonic interference suppression filter that demonstrate a stopband of 1% of center frequency, with very small shape factors, and wide-band transmission with very low passband ripples, for high-resolution interference mitigation in fiber-based transmission systems.

This paper is organized as follows. The new high-resolution large FSR photonic interference mitigation filter topology is presented in Section II. The analysis and design are described in Section III. Finally, Section IV describes experimental results on the large FSR interference suppression photonic filter, which demonstrates the high-resolution notch filtering and wide passband.

II. Large FSR Photonic Notch Filter Topology

The topology of the new large FSR photonic notch filter is shown in Fig. 1. A multiple-wavelength RF modulated signal is split into two parallel arms. The signal is routed via a direct fiber path, shown in the top part of Fig. 1, and a parallel path, which contains two offset cavity high-Q optical bandpass filters and a cascade of unbalanced delay line structures, shown in the lower part of Fig. 1. In this structure, a new technique is introduced to realize a dual-cavity noncommensurate delay line bandpass filter [10] to obtain a square type of response. This is based on a novel wavelength-division multiplexing (WDM) approach using multiple wavelengths and grating-based cavities centered at the different wavelengths. The two wavelength cavities are shown in Fig. 1. The length difference $2\Delta L$ between the two cavities is optimized to achieve a combined bandpass response that has a square type of characteristic. In comparison to previous structures [10] that used one arm for each cavity, the new multiple-wavelength structure has the advantage that it can coalesce multiple cavities into a single arm. Moreover, all the cavities share the same erbium-doped fiber amplifier (EDFA), and this reduces the requirement for matching the EDFA gain for each cavity. Finally, and most importantly, because all the cavities share the same gain, any variation in the gain affects all the cavities in synchronism, so that the overall combined bandpass filter response of the cavities maintains its shape and provides a robust characteristic even in the face of pump power and gain fluctuations.

The multiple-wavelength bandpass filters not only have the desired response at the fundamental frequency f_0 but also have a recursive response at lf_0, where l is an integer. After subsequent subtraction from the direct arm response, this recursive

Manuscript received April 16, 2003; revised September 2, 2003. This work was supported by the Australian Research Council.

The authors are with the School of Electrical and Information Engineering and Australian Photonics CRC, University of Sydney, 2006 N.S.W., Australia.

Digital Object Identifier 10.1109/JLT.2003.820039

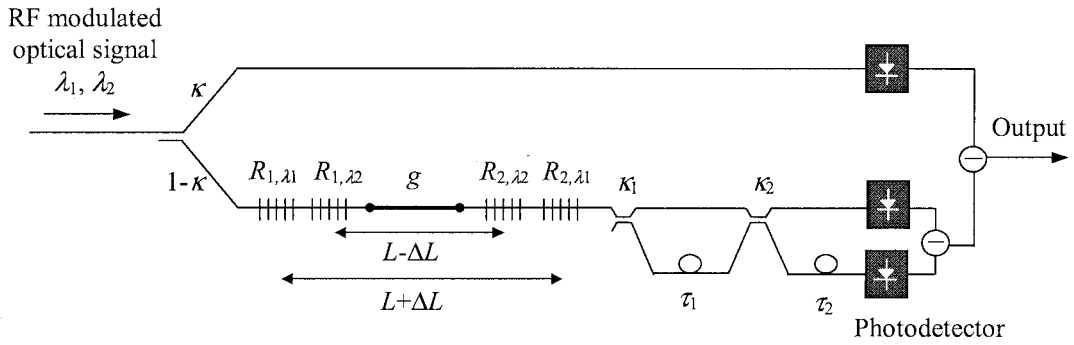

Fig. 1. The topology of the new fiber-based large FSR filter for interference mitigation.

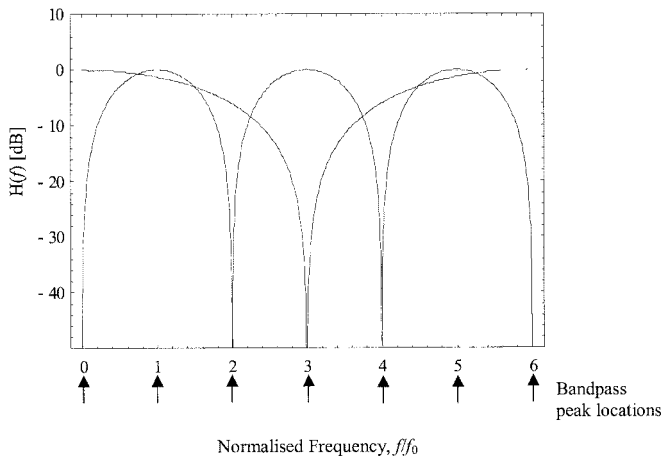

Fig. 2. Frequency response of the MZ notch filter and the balanced detection notch filter.

response generates additional, unwanted notches at lf_0, which come into effect at higher frequencies and hence limit the spectral width of the passband. To solve this problem, we introduce a new delay-line structure following the WDM filters, as shown in Fig. 1. This comprises a cascade of unbalanced delay lines, which have delay differences τ_1 and τ_2. The idea is to introduce a series of notches that suppress several harmonic responses of the multiple-wavelength bandpass filter. Hence after subtraction of the combined signal from the all-pass arm, the desired notch at f_0 is realized. However, the potential notches at several harmonics are suppressed, and the passband is significantly extended.

The unbalanced delay structure with delay difference τ_1 forms a fiber-optic filter with the notches at $(0.5+m)$/FSR, where m is an integer. We design the length difference to be three times shorter than the cavity length of the bandpass filter; hence the FSR of this notch filter becomes six times the bandpass filter FSR. Thus the fundamental notch produced by this filter coincides with the third harmonic of the bandpass filter response, as shown in Fig. 2. The next unbalanced delay structure with delay difference τ_2 feeding into the balanced detector forms another fiber-optic filter with notches at m/FSR. We design the fiber length difference in this structure to be the same as the cavity length of the bandpass filter; hence the FSR of this notch filter is twice the bandpass filter FSR. Therefore the notches produced by this filter occur at dc and all even harmonics of the bandpass filter response, as shown in Fig. 2. The overall effect of the unbalanced delay line filters is to pass the fundamental bandpass filter response but to eliminate the peaks at dc, second, third, and fourth passband harmonics of the bandpass filter response. Hence after subtraction of the combined signal from the all-pass arm, the desired notch at f_0 is realized. However, the potential notches at $2f_0$, $3f_0$, and $4f_0$ are eliminated, and the passband and FSR of the filter are increased fourfold.

III. Analysis and Design

The transfer function of the filter in Fig. 1 is given by

$$\begin{aligned} H(z) = {} & \kappa z^{-\frac{1}{2n_1}} - \{(1-\kappa)g(1-R_1)(1-R_2) \\ & \times \left[\frac{1}{1-Uz^{k-1}} + \frac{1}{1-Uz^{-k-1}}\right] \\ & \times \left[(1-\kappa_1)(1-\kappa_2) + \kappa_1\kappa_2 z^{-\frac{1}{n_1}}\right] \\ & \times \left[2\left((1-\kappa_2) - \kappa_2 z^{-\frac{1}{n_2}}\right)\right]\} \end{aligned} \quad (1)$$

where $U = g^2R_1R_2$, g is the gain of the EDFA, R_1 and R_2 are the grating reflectivities, κ, κ_1, and κ_2 are the optical coupler coupling ratios, $k = \Delta L/L$, n_1 is the ratio of the Mach–Zehnder (MZ) filter FSR to the bandpass filter FSR, n_2 is the ratio of the balanced detection filter FSR to the bandpass filter FSR, $z = \exp(j2\pi Tf)$, f is the RF frequency, $T = (2nL)/c$ is the round-trip delay time corresponding to the cavity length L that is used to set the filter center frequency, n is the fiber refractive index, and c is the speed of light. Note that in contrast to [11], balanced detection is used at the output of the τ_2 filter; hence a factor of two appears in the last term in (1). This shows that the present filter topology with balanced detection has the advantage of utilizing all the signal paths, thus avoiding any efficiency loss. Moreover, another feature of the balanced detection scheme utilized is that the bandpass peak at dc is eliminated; hence the overall notch filter passband response is not compromised at low frequencies.

For simplicity, we can ensure that the direct path arm can be implemented with just a length of fiber, and hence we design the direct pass signal to have the same amplitude as the bandpass filter passband amplitude. Analysis shows that the required value of optical coupling ratio to achieve this is given by (2) as shown at the bottom of the next page.

The RF frequency f in (2) is $1/T$, which corresponds to the notch frequency. Note that the coupling ratio of the optical coupler can only be used to control the amplitude of the two arms. However, the signals that are detected from the two arms have both magnitude and phase characteristics. The RF phase characteristic of the signal at the notch frequency for the two arms must also be matched in order to obtain complete cancellation of the signals at the fundamental frequency to produce a deep notch. In particular, the MZ filter stage introduces a nonzero phase at the notch frequency. This additional phase can be matched by introducing an additional length into the direct path arm. Hence, unlike the case in [10], here the lengths of the two arms are designed to be different, in order to equalize the phase introduced by the unbalanced filter that is used to extend the FSR. Our analysis has found that with the inclusion of an additional length in the all-pass arm, this condition of phase matching of the two arms could be met. The required length of the all-pass arm L_1 to achieve this is given by

$$L_1 = L_2 + \frac{L}{6} \tag{3}$$

where L_2 is the minimum path length of the lower arm.

Finally, the delay length of the active section L is chosen to give a delay time corresponding to the filter design center frequency f_0

$$L = \frac{c}{2nf_0} \tag{4}$$

and the relative delay times of the unbalanced delay line filters are chosen to be

$$\tau_1 = \frac{1}{6f_0} \tag{5}$$

and

$$\tau_2 = \frac{1}{2f_0}. \tag{6}$$

It may be seen that the impulse response for a pulse into the bandpass filter followed by the unbalanced delay line filters shows that it is not possible for two pulses to arrive at the photodetector simultaneously, which means there are no two paths in this structure with the same length. Hence, the use of a laser whose coherence length is less than the minimum delay path difference in the structure, i.e., τ_1, ensures that there are no coherent interference effects. Finally, the wavelength separation of the carriers λ_1 and λ_2 is chosen to be large enough so that beat frequency components at the photodetector fall well outside the RF passband.

As an example, we consider the design of an interference rejection filter having 1% bandwidth of the center frequency at 1.5 GHz, i.e., having a -6 dB stopband width of 15 MHz.

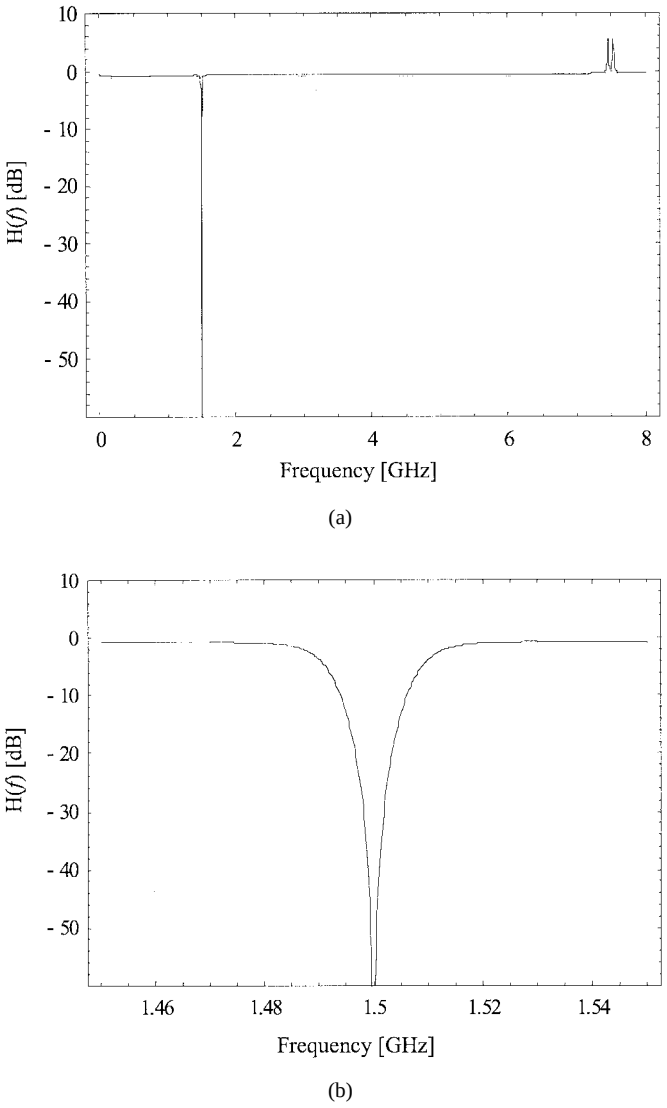

Fig. 3. Frequency response of the large FSR dual-cavity photonic interference rejection filter: (a) wide-band response and (b) detailed section of response within 100 MHz of center stopband frequency.

In order to meet these requirements, the dual-cavity structure was designed with grating reflectivities of $R_1 = R_2 = 0.5$, fractional length detuning factor $k = 0.0048$, erbium amplifier single-pass gain of $g = 1.97$, and coupler coupling ratio $\kappa_1 = \kappa_2 = 0.5$. The input coupler's coupling ratio κ is 93.5%. The frequency response of this fiber-based interference rejection filter is shown in Fig. 3. The notch frequency is at 1.5 GHz. The passband is flat within 0.1 dB, and the passband transmission factor has less than 1 dB loss. We have investigated the tolerance of the FSR extension using cascaded delay line filters,

$$\kappa = \frac{\left|g(1-R_1)(1-R_2)\left[\frac{1}{1-Uz^{k-1}}+\frac{1}{1-Uz^{-k-1}}\right]\cdot\left[(1-\kappa_1)(1-\kappa_2)+\kappa_1\kappa_2 z^{-\frac{1}{n_1}}\right]\cdot\left[2\left((1-\kappa_2)-\kappa_2 z^{-\frac{1}{n_2}}\right)\right]\right|}{\left\{1+\left|g(1-R_1)(1-R_2)\left[\frac{1}{1-Uz^{k-1}}+\frac{1}{1-Uz^{-k-1}}\right]\cdot\left[(1-\kappa_1)(1-\kappa_2)+\kappa_1\kappa_2 z^{-\frac{1}{n_1}}\right]\cdot\left[2\left((1-\kappa_2)-\kappa_2 z^{-\frac{1}{n_2}}\right)\right]\right|\right\}} \tag{2}$$

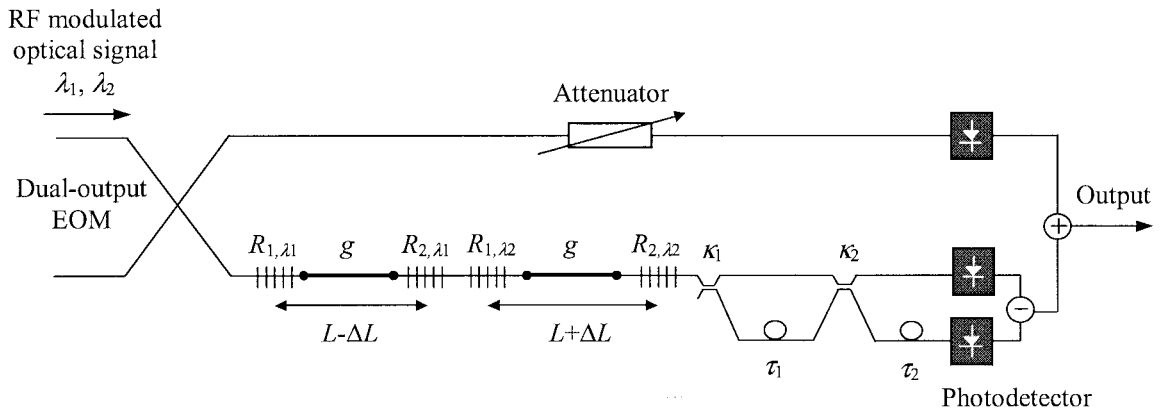

Fig. 4. Experimental setup of the new fiber-based large FSR filter for interference mitigation.

with regard to passband ripples around the harmonic frequencies. High Q-values of the bandpass filter do not pose an issue because they can readily fit within the relatively wide notch width of the two-tap notch filters, and hence they can be effectively suppressed so that when subtracted from the all-pass arm, negligible ripples result at harmonic frequencies. What is more important is that the delay times τ_1 and τ_2 are accurate so that the notches of the two-tap filters are aligned in frequency with the harmonic bandpass responses. However, a tolerance analysis shows that to keep ripples below 0.5 dB around harmonic frequencies, the tolerance on τ_1 and τ_2 needs to be within 3%, which is practical.

We have also investigated the accuracy that is required in the additional length needed in the all-pass arm to match the RF phase between the two arms. It was found that if the additional length is not $L/6$, which is optimum, there is some reduction in the notch depth. However for a 1% change in the additional length from its optimum length, a notch depth of over 46 dB could still be obtained. Moreover, this change has very little effect on the filter passband flatness. The amount of the passband loss or gain can be controlled by the choice of grating reflectivity and EDFA gain in the bandpass filter. We have investigated the effect of the EDFA noise, since there are multiple recirculations in the cavity. An analysis of the signal-spontaneous beat noise and the spontaneous–spontaneous beat noise in an amplified recirculating delay line [12] shows that these noise elements peak at the bandpass frequency; however, they are quite low in the out-of-band frequency regions. For the EDFA gain and cavity reflection parameters used here, it was found that in the out-of-band frequency regions, these noise values are 35 dB lower than at the peak. Since the passband of the notch filter corresponds to the out-of-band regions of the bandpass filters, the noise added by the EDFA in the passband of the notch filter is quite low.

The frequency response of this fiber-based interference rejection filter, in Fig. 3, shows that the lower transmission band is from dc to 1.5 GHz and the upper transmission band is from 1.5 to 7.5 GHz. This demonstrates the cancellation of the intermediate notches, which largely increases the system bandwidth. Two small unwanted peaks are observed at 7.5 GHz because the delay-line notch filter response does not cover the fifth harmonic of the bandpass filter passband and the direct pass phase at this frequency is different to the bottom path. A detailed section of the frequency response, within 100 MHz of the center stopband frequency, is displayed in Fig. 3(b). The 6-dB width of the stopband of the filter is 15 MHz. The shape factor, defined as the ratio of the -6 dB bandwidth to the -35 dB bandwidth of the interference rejection filter, is 5.8 for this structure. This achieves both a very low shape factor and a four-times FSR increase compared to the conventional existing structures. This demonstrates that the novel WDM notch filter can simultaneously provide a small shape factor and a large FSR frequency response. It can be noted that the structure of Fig. 1 is quite general. The key aspect of enabling a multifold increase in the FSR of the interference rejection filter is not dependent on the number of wavelengths used. For instance, if only a single wavelength is available in some applications, the FSR would still be increased in the same way, and if a good shape factor is also required, then separate cavities in parallel could be used for each bandpass filter. Alternatively, if several wavelengths are available, this is useful in simplifying the topology so that the multiple cavities can be coalesced into one arm. However, the operation is the same. Also, by increasing the number of wavelengths, additional offset cavities within the same topology can be realized to further reduce the shape factor of the interference rejection filter—e.g., using three wavelengths, the shape factor can be reduced to 2.7. In addition, increasing the number of unbalanced delay line filter stages to p stages, the passband FSR of the interference rejection filter can be increased by a factor of 2^p.

IV. Experiment and Results

To verify the proof of principle for the new topology, the filter structure was set up experimentally. The experiments were carried out for a relatively low notch design center frequency of 60 MHz for simplicity and ease of measurement; however, they provided a demonstration to verify the concepts. The photonic interference rejection filter was designed to have a notch bandwidth of 1% of center frequency, and four times increase in passband FSR.

Fig. 4 shows the experimental setup. The two wavelengths used were 1536 and 1541 nm, and the coherence of the sources

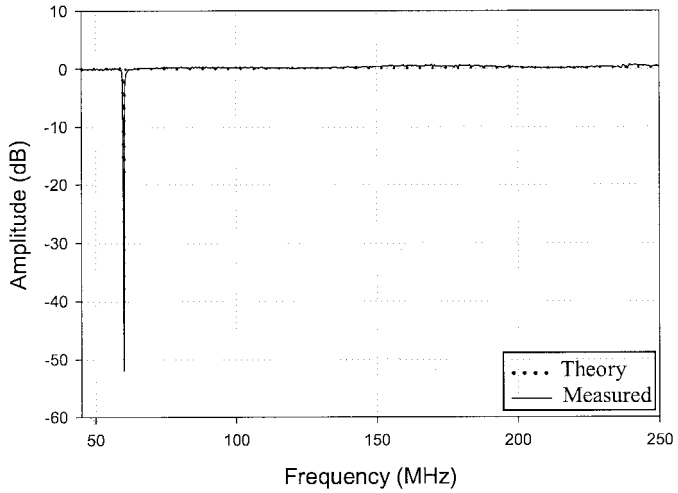

(a)

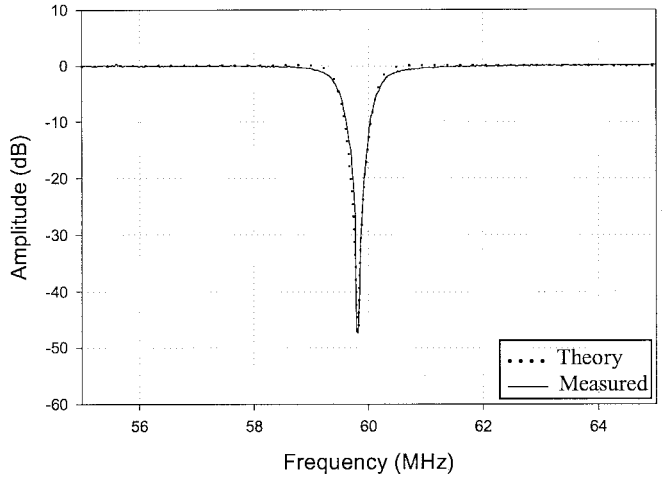

(b)

Fig. 5. Comparison between the measured and predicted frequency response for the large FSR dual-cavity photonic interference rejection filter: (a) wide-band response and (b) detailed section of response within 10-MHz span around the center stopband frequency.

was smaller than the minimum delay time difference in the structure. The two wavelengths were combined with a 3-dB coupler and were modulated in a dual-output electrooptic modulator, one arm of which fed into the all-pass arm, which had a small variable attenuator to balance the amplitude, and the other arm of which fed into the dual-cavity filter. Instead of using two superimposed offset grating cavities, which we lacked, we realized the dual-cavity structure by implementing each wavelength cavity separately with 50% reflectivity gratings and connecting them in series, as shown in Fig. 4. The length of each cavity was 1.682 and 1.664 m, which yields an offset factor of $k = \Delta L/L = 0.0053$, and a center frequency at 60 MHz. The pump signal was split to pump the erbium-doped fiber in each cavity. The EDFA gain was set to 1.971 for both cavities. The delay length difference of the unbalanced delay line filters were 0.567 and 1.689 m. Since the dual-output modulator provides two out-of-phase modulated signals, one into the direct path and the other into the lower arm, at the output the electric currents were added after photodetection.

A comparison between the measured and predicted frequency response for the high-performance WDM notch filter is shown in Fig. 5. Fig. 5(a) shows the wide-band response, and these results demonstrate that the potential periodic recursive notch responses at 120, 180, and 240 MHz have been eliminated. The next unwanted harmonic response occurs at 300 MHz. As a result, the FSR of the passband has been increased by a factor of four. The measurements also show a very flat passband with <0.5 dB ripple. Fig. 5(b) shows a detailed response of the filter within a 10-MHz range of its center frequency. The measured shape factor of this filter is 8.7. This demonstrates that the novel WDM structure has the ability of producing both a small shape factor and a large FSR notch filter response. Excellent agreement can be seen between the measured and predicted frequency response of the interference suppression filter.

V. Conclusion

A new topology for a photonic signal processor, which overcomes the basic recursive frequency response problem that limits the realizable width of the passband range, has been presented. The topology is based on a new multiple-wavelength offset-cavity structure that is cascaded with a series of unbalanced delay line structures. This not only can synthesize a very narrow notch response with good shape factor but also permits a multifold extension of the FSR and passband width, and also maintains the filter passband to low frequencies. It enables both a high-resolution interference suppression filter and a very wide passband to be obtained. The analysis and design procedure for the filter has been described. The new filter topology has been experimentally verified, and results have been presented for this photonic interference suppression filter that demonstrate a stopband of 1% of center frequency and realize a fourfold increase in the FSR and passband width while also having a very small shape factor of 8.7 and very low passband ripples. This is important for narrow excision of RF interference while simultaneously transmitting the wanted signal over a flat and wide passband, and offers built-in high-resolution interference mitigation capabilities in fiber-based transmission systems.

References

[1] D. B. Hunter and R. A. Minasian, "Reflectively tapped fiber optic transversal filter using in-fiber Bragg gratings," *Electron. Lett.*, vol. 31, no. 12, pp. 1010–1012, 1995.

[2] J. Capmany, D. Pastor, and B. Ortega, "New and flexible fiber-optic delay-line filters using chirped Bragg gratings and laser arrays," *IEEE Trans. Microwave Theory Tech.*, vol. 47, pp. 1321–1326, July 1999.

[3] F. Coppinger, S. Yegnanarayanan, P. D. Trinh, and B. Jalali, "Continuously tunable photonic radio-frequency notch filter," *IEEE Photon. Technol. Lett.*, vol. 9, pp. 339–341, Mar. 1997.

[4] W. Zhang, J. A. R. Williams, L. A. Everall, and I. Bennion, "Fiber optic radio frequency notch filter with linear and continuous tuning by using a chirped fiber grating," *Electron. Lett.*, vol. 34, no. 18, pp. 1770–1772, 1998.

[5] S. Li, K. S. Chiang, W. A. Gambling, Y. Liu, L. Zhang, and I. Bennion, "A novel tunable all-optical incoherent negative-tap fiber-optic transversal filter based on a DFB laser diode and fiber Bragg gratings," *IEEE Photon. Technol. Lett.*, vol. 12, pp. 1207–1209, Sept. 2000.

[6] J. Marti, V. Polo, F. Ramos, and D. Moodie, "Photonic tunable microwave filters employing electroabsorption modulators and wideband chirped fiber gratings," *Electron. Lett.*, vol. 35, no. 4, pp. 305–306, 1999.

[7] E. H. W. Chan, K. E. Alameh, and R. A. Minasian, "Photonic bandpass filters with high skirt selectivity and stopband attenuation," *J. Lightwave Technol.*, vol. 20, pp. 1962–1967, Nov. 2002.
[8] T. A. Cusick, S. Iezekiel, R. E. Miles, S. Sales, and J. Capmany, "Synthesis of all-optical microwave filters using Mach-Zehnder lattices," *IEEE Trans. Microwave Theory Tech.*, vol. 45, pp. 1458–1462, Aug. 1997.
[9] J. X. Chen, Y. Wu, J. Hodiak, and P. K. L. Yu, "A novel digitally tunable microwave-photonic notch filter using differential group-delay module," *IEEE Photon. Technol. Lett.*, vol. 15, pp. 284–286, Feb. 2003.
[10] R. A. Minasian, K. E. Alameh, and E. H. W. Chan, "Photonic-based interference mitigation filters," *IEEE Trans. Microwave Theory Tech.*, vol. 49, pp. 1894–1899, Oct. 2001.
[11] N. You and R. A. Minasian, "A novel high-Q optical microwave processor using hybrid delay-line filters," *IEEE Trans. Microwave Theory Tech.*, vol. 47, pp. 1304–1308, July 1999.
[12] J. Kringlebotn and K. Bloktecjar, "Noise analysis of an amplified fiber-optic recirculating-ring delay line," *J. Lightwave Technol.*, vol. 12, pp. 573–582, Mar. 1994.

E. H. W. Chan received the B.Sc. and B.Eng. degrees in information system electrical engineering (with honors) from the University of Sydney, N.S.W., Australia, in 1998 and 2000, respectively, and is currently working toward the Ph.D. degree at the University of Sydney.

His research interests include communications technology (optical, microwave, radio frequency), lightwave networks and optical fiber communications, optical signal processing, and photonic and microwave technology.

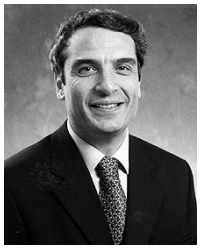

R. A. Minasian (S'78–M'80–SM'00–F'03) received the B.E. degree from the University of Melbourne, Melbourne, Australia, the M.Sc. degree from the University of London, University College, London, U.K., and the Ph.D. degree from the University of Melbourne.

He is currently a Professor and holds a Personal Chair with the School of Electrical and Information Engineering, University of Sydney, Sydney, Australia, and is Director of the Fiber-Optics and Photonics Research Group. His research encompasses optical telecommunications and signal processing and currently centers on photonic signal processing, broad-band optical communications, microwave photonics, and optical phased arrays. He has contributed to more than 170 technical publications in these areas. He is an Associate Editor of *Optical Fiber Technology*.

Prof. Minasian is a Fellow of the Institute of Engineers, Australia, and a Member of the Technical Committee on Microwave Photonics of the IEEE Microwave Theory and Techniques Society (IEEE MTT-S) and has served on the program committees for several international conferences, including the IEEE International Meeting on Microwave Photonics (MWP 2000, and MWP 2003) and the Asia Pacific Microwave Conference (APMC 2000). He was the recipient of the ATERB Medal for Outstanding Investigator in Telecommunications, awarded by the Australian Telecommunications and Electronics Research Board.